Modeling and Iterative Learning Control of a Circular Deformable Mirror ⋆

Błażem Cichy * **Petr Augusta** ** **Krzysztof Gałkowski** *
Andreas Rauh *** **Harald Aschemann** *** **Eric Rogers** ****
Branislav Rehák **

* *Institute of Control and Computation Engineering, University of Zielona Góra, ul. Szafrana 2, 65-516 Zielona Góra, Poland, (e-mail: {B.Cichy, K.Galkowski}@issi.uz.zgora.pl).*
** *Institute of Information Theory and Automation, The Czech Academy of Sciences, Pod Vodárenskou věží 4, CZ-182 08 Prague, Czech Republic, (e-mail: {augusta, rehakb}@utia.cas.cz)*
*** *Chair of Mechatronics, University of Rostock, Justus-von-Liebig-Weg 6, D-18059 Rostock, Germany, (e-mail: {Andreas.Rauh, Harald.Aschemann}@uni-rostock.de)*
**** *Dept. of Electronics and Computer Science, University of Southampton, Southampton SO17 1BJ, UK, (e-mail: etar@ecs.soton.ac.uk)*

Abstract: An unconditionally stable finite difference scheme for systems whose dynamics are described by a fourth-order partial differential equation is developed with the use of a regular hexagonal grid. The scheme is motivated by the well-known *Crank-Nicolson* discretization that was originally developed for second-order systems and it is used to develop a discrete in time and space model of a deformable mirror as a basis for control law design. The obtained model is used for a control design via iterative learning control and supporting numerical simulations are given.

Keywords: Five to ten keywords, preferably chosen from the IFAC keyword list.

1. INTRODUCTION

Discretization of partial differential equations (PDE) describing systems with spatial and temporal dynamics is required to obtain discrete models that can form a basis for the design and digital implementation of control laws. A critical factor for this general approach is numerical stability, i.e., the discrete approximation must produce trajectories close to those produced by the PDE and identical stability properties. One group of methods which can be applied to the discretization of PDEs are based on a finite difference approximation (Strikwerda, 1989).

Discretization of PDEs describing systems or processes with one temporal and one spatial variable, such as the one-dimensional heat transfer equation, results in models that are very similar to repetitive processes (Rogers et al., 2007). The unique characteristic of a repetitive process is a series of sweeps, termed passes, through a set of dynamics defined over a fixed finite duration known as the pass length. In particular, a pass is completed and then the process is reset to the starting location and the next pass can begin, either immediately after the resetting is complete or after a further period of time has elapsed. On each pass, an output, termed the pass profile, is produced which acts as a forcing function on, and hence contributes to, the dynamics of the next pass profile. Repetitive processes are therefore a particular case of 2D systems where there are two independent directions of the information propagation.

In the repetitive process representation of the discretization of PDEs, the pass number is associated with the discrete time sample instants and the along pass dynamics are governed by the discrete spatial variable, see, e.g., (Cichy et al., 2011). One class of the finite difference discretization schemes currently available are those known as explicit (Rabenstein and Steffen, 2011), which were used by (Cichy et al., 2011). These methods produce a causal in time discrete recursive model where at any instant on the current pass a window of sample instants on the previous pass contributes to the dynamics. Such models are known as wave discrete linear repetitive processes and include the extensively studied standard discrete linear repetitive processes as a special case, i.e., when the previous pass contribution at time instant p on the current pass only comes from the same instant on the previous pass.

Explicit discretization methods are conditionally numerically stable, i.e., the time discretization period is related to its spatial counterpart, which, in effect, leads to the need to use dense time and spatial discretization grids. One way of overcoming this drawback is to use the so-called singular

⋆ This work is partially supported by National Science Centre in Poland, grant No. 2015/17/B/ST7/03703.

methods, see (Rabenstein and Steffen, 2011, 2009) and, in particular, the Crank-Nicolson method (Crank and Nicolson, 1947), which frequently produces an unconditionally stable discrete approximation to the dynamics of the original PDE. Hence, the temporal and spatial grids become independent and can therefore be less dense. However, the resulting discrete model is in implicit form, i.e., there is no straightforward dependence of the pass profile at any instance on the current pass and the window of previous pass values. Instead, this dependence is between windows of data points on the current and previous passes.

The simplest way of formulating and solving control problems for singular systems of the considered class requires the use of the lifting approach, i.e., absorbing the spatial structure of the system into possibly high dimensional vectors, see, e.g., (Cichy et al., 2012) for a detailed treatment. In this paper, the Crank-Nicolson method is extended to systems described by PDEs defined over time and two space variables. As a particular example, a thin flexible plate is considered, which, e.g., can be used to model the vibrations of a deformable mirror subject to a transverse external force. In contrast to (Augusta et al., 2015), a circular plate is considered and a regular hexagonal grid is used for discretization.

Previous results (Augusta et al., 2016) can be applied to show that the resulting discrete approximation has the unconditional numerical stability property and hence, relative to the discrete approximations discussed above, a significantly less dense discretization grid can be used with negligible degradation of the approximate model dynamics. This, in turn, means a much smaller number of sensors and actuators distributed over a controlled plate can be used with advantages in terms of control law design and implementation. As one possible option given a discrete model, an iterative learning control law is designed to achieve a given spatial/temporal reference signal and supporting numerical simulations given.

2. PARTIAL DIFFERENTIAL EQUATION REPRESENTATION

The dynamics of the continuous deformable mirror considered in this work are modeled by the following Lagrangian PDE

$$\frac{\partial^4 w(t,x,y)}{\partial x^4} + 2\,\frac{\partial^4 w(t,x,y)}{\partial x^2\,\partial y^2} + \frac{\partial^4 w(t,x,y)}{\partial y^4} + \frac{\rho}{D}\,\frac{\partial^2 w(t,x,y)}{\partial t^2} = \frac{f(t,x,y)}{D}, \quad (1)$$

where

w is the lateral deflection in the z direction [m],
ρ is the mass per unit area [$\mathrm{kg\,m^{-2}}$],
f is the transverse external force, with dimension of force per unit area [$\mathrm{N\,m^{-2}}$],
$\frac{\partial^2 w}{\partial t^2}$ is the acceleration in the z direction [$\mathrm{m\,s^{-2}}$],
$D = E\,h^3/(12\,(1-\nu^2))$,
ν is the Poisson ratio,
h is the thickness of the plate [m],
E is Young's Modulus [$\mathrm{N\,m^{-2}}$].

Further background on (1) can be found in, e.g., (Timoshenko and Woinowski-Krieger, 1959). Also control action based on an array of actuators and sensors is considered. The sensors are distributed over the entire surface of the plate of the diameter a, but the actuators are only used on the plate central part with diameter $d < a$. The load hence can be modeled with a Heaviside function H as

$$f(t,x,y) = \left(1 - H(x^2+y^2-d^2)\right)\, q(t,x,y).$$

Since the function $1 - H(x^2+y^2-d^2)$ is always one within the region where the load is applied, the distributed system input is set to $f(t,x,y) = q(t,x,y)$ in the corresponding subregion of radius d and to $f(t;x;y) = 0$ outside.

To derive a model suitable for control design, the use of an actuator array requires the discretization of (1) in the spatial variables. Moreover, since the control will be implemented digitally, (1) must also be discretized with respect to time. This task is considered next.

3. DISCRETIZATION AND MODELING

The discretization of (1) is based on finite difference methods, where, in general terms, the following steps must be implemented:

(1) cover the region where a solution is sought by a regular grid, i.e., a regular mesh of nodal points,
(2) replace the derivative terms in the PDE by differences using only values at nodal points, i.e., approximate the derivatives.

To complete these tasks, an implicit discretization of the Crank-Nicolson form will be used. Such a discretization results in an unconditionally numerically stable approximation of the system dynamics, see (Augusta et al., 2016) for a full treatment.

Let p, l, m denote the time instant t_p and the coordinates of nodal points x_l, y_m, respectively. Consider a circular deformable mirror with a regular hexagonal grid used. Also let the number of nodal points on the plate diagonal be an odd number denoted by n. Then, the number of all nodal points is $N = \frac{3\,n^2+1}{4}$.

In the discretization method used, derivatives arising in (1) are replaced by finite differences as follows

$$\begin{aligned}\frac{\partial^4 w}{\partial x^4} \approx \frac{1}{4\,\delta_x^4}\big(& w_{p+2,l+2,m} - 2\,w_{p+2,l+1,m+1} - 2\,w_{p+2,l+1,m-1} \\ &+ 6\,w_{p+2,l,m} - 2\,w_{p+2,l-1,m+1} - 2\,w_{p+2,l-1,m+1} \\ &+ w_{p+2,l-2,m} + 2\,w_{p+1,l+2,m} - 4\,w_{p+1,l+1,m+1} \\ &- 4\,w_{p+1,l+1,m-1} + 12\,w_{p+1,l,m} - 4\,w_{p+1,l-1,m+1} \\ &- 4\,w_{p+1,l-1,m+1} + 2\,w_{p+1,l-2,m} + w_{p,l+2,m} \\ &- 2\,w_{p,l+1,m+1} - 2\,w_{p,l+1,m-1} + 6\,w_{p,l,m} \\ &- 2\,w_{p,l-1,m+1} - 2\,w_{p,l-1,m+1} + w_{p,l-2,m}\big), \end{aligned} \quad (2)$$

$$
\begin{aligned}
\frac{\partial^4 w}{\partial y^4} \approx \frac{1}{4\,\delta_y^4}\big(& w_{p+2,l,m+2} - 2\,w_{p+2,l+1,m+1} - 2\,w_{p+2,l-1,m+1} \\
&+ 6\,w_{p+2,l,m} - 2\,w_{p+2,l+1,m-1} - 2\,w_{p+2,l+1,m-1} \\
&+ w_{p+2,l,m-2} + 2\,w_{p+1,l,m+2} - 4\,w_{p+1,l+1,m+1} \\
&- 4\,w_{p+1,l-1,m+1} + 12\,w_{p+1,l,m} - 4\,w_{p+1,l+1,m-1} \\
&- 4\,w_{p+1,l+1,m-1} + 2\,w_{p+1,l,m-2} + w_{p,l,m+2} \\
&- 2\,w_{p,l+1,m+1} - 2\,w_{p,l-1,m+1} + 6\,w_{p,l,m} \\
&- 2\,w_{p,l+1,m-1} - 2\,w_{p,l+1,m-1} + w_{p,l,m-2}\big), \qquad (3)
\end{aligned}
$$

$$
\begin{aligned}
\frac{\partial^4 w}{\partial x^2 \partial y^2} \approx \frac{1}{4\,\delta_x^2\,\delta_y^2}\big(& - w_{p+2,l+1,m+1} - w_{p+2,l+1,m-1} \\
&+ 4\,w_{p+2,l,m} - w_{p+2,l-1,m+1} - w_{p+2,l-1,m-1} \\
&- 2\,w_{p+1,l+1,m+1} - 2\,w_{p+1,l+1,m-1} + 8\,w_{p+2,l,m} \\
-2\,w_{p+2,l-1,m+1} - 2\,w_{p+2,l-1,m-1} &- w_{p,l+1,m+1} - w_{p,l+1,m-1} \\
&+ 4\,w_{p,l,m} - w_{p,l-1,m+1} - w_{p,l-1,m-1}\big), \qquad (4)
\end{aligned}
$$

$$
\frac{\partial^2 w}{\partial t^2} \approx \frac{1}{\delta_t^2}\big(w_{p+2,l,m} - 2\,w_{p+1,l,m} + w_{p,l,m}\big), \qquad (5)
$$

where δ_x and δ_y denote the distances between the nodes in the x and y directions, respectively, and δ_t denotes the temporal sampling period. Substituting (2)–(5) into (1) followed by routine manipulations gives the following partial recurrence equation as a discrete model of the original PDE (1)

$$
\begin{aligned}
&\left(\frac{1}{4\,\delta_x^4}\right)\big(w_{p+2,l+2,m} + w_{p+2,l-2,m}\big) \\
&+\left(-\frac{1}{2\,\delta_x^4} - \frac{1}{2\,\delta_y^4} - \frac{1}{2\,\delta_x^2\,\delta_y^2}\right)\big(w_{p+2,l+1,m+1} \\
&\quad + w_{p+2,l+1,m-1} + w_{p+2,l-1,m+1} + w_{p+2,l-1,m-1}\big) \\
&+\left(\frac{1}{4\,\delta_y^4}\right)\big(w_{p+2,l,m+2} + w_{p+2,l,m-2}\big) \\
&+\left(\frac{3}{2\,\delta_x^4} + \frac{3}{2\,\delta_y^4} + \frac{2}{\delta_x^2\,\delta_y^2} + \frac{\rho}{D\,\delta_t^2}\right) w_{p+2,l,m} \\
&+\left(\frac{1}{2\,\delta_x^4}\right)\big(w_{p+1,l+2,m} + w_{p+1,l-2,m}\big) \\
&+\left(-\frac{1}{\delta_x^4} - \frac{1}{\delta_y^4} - \frac{1}{\delta_x^2\,\delta_y^2}\right)\big(w_{p+1,l+1,m+1} \\
&\quad + w_{p+1,l+1,m-1} + w_{p+1,l-1,m+1} + w_{p+1,l-1,m-1}\big) \qquad (6) \\
&+\left(\frac{1}{2\,\delta_y^4}\right)\big(w_{p+1,l,m+2} + w_{p+1,l,m-2}\big) \\
&+\left(\frac{3}{\delta_x^4} + \frac{3}{\delta_y^4} + \frac{4}{\delta_x^2\,\delta_y^2} - \frac{2\,\rho}{D\,\delta_t^2}\right) w_{p+1,l,m} \\
&+\left(\frac{1}{4\,\delta_x^4}\right)\big(w_{p,l+2,m} + w_{p,l-2,m}\big) \\
&+\left(-\frac{1}{2\,\delta_x^4} - \frac{1}{2\,\delta_y^4} - \frac{1}{2\,\delta_x^2\,\delta_y^2}\right)\big(w_{p,l+1,m+1} \\
&\quad + w_{p,l+1,m-1} + w_{p,l-1,m+1} + w_{p,l-1,m-1}\big) \\
&+\left(\frac{1}{4\,\delta_y^4}\right)\big(w_{p,l,m+2} + w_{p,l,m-2}\big) \\
&+\left(\frac{3}{2\,\delta_x^4} + \frac{3}{2\,\delta_y^4} + \frac{2}{\delta_x^2\,\delta_y^2} + \frac{\rho}{D\,\delta_t^2}\right) w_{p,l,m} = \frac{1}{D} q_{p,l,m}.
\end{aligned}
$$

This equation is the planar equivalent of a singular wave repetitive process, which is second order in the discrete

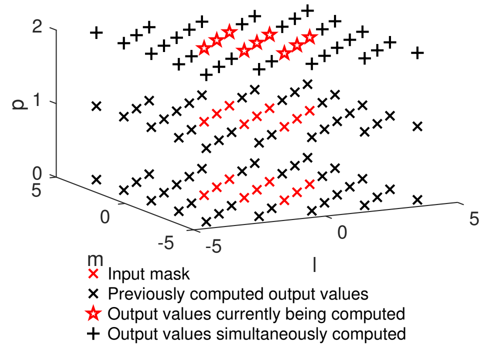

Fig. 1. Computation mask associated with the partial recurrence equation (6).

time variable p and gives the dependence between the windows $(l-2, m+2), \ldots, (l+2, m+2), \ldots, (l-2, m-2), \ldots, (l+2, m-2)$ at the time instant $p+2$ and the same rectangles at the two preceding time instants, i.e., $p+1$ and p respectively. This is illustrated by the computation mask shown in Fig. 1. Moreover, $q_{p,l,m}$ can be considered as a distributed control signal, acting independently at each of the nodal points, to the system.

At this stage, (6) can be written in the form

$$
A\,W_{p+2} + B\,W_{p+1} + A\,W_p = C\,Q_p, \qquad (7)
$$

where $p \geq 0$ and W_p and Q_p are vectors of the deflections and external forces at the nodal points, respectively, i.e.,

$$
W_p = \begin{bmatrix} w_{p,1} \\ w_{p,2} \\ \vdots \\ w_{p,N} \end{bmatrix}, \quad Q_p = \begin{bmatrix} q_{p,1} \\ q_{p,2} \\ \vdots \\ q_{p,N} \end{bmatrix},
$$

and A, B and C are Toeplitz matrices constructed from the coefficients of (6). Since the deflections at all boundary nodal points and those external to the plate are always zero, these are not included in W_p; similarly for Q_p. Also (7) can be written as

$$
W_{p+2} = -A^{-1}\,B\,W_{p+1} - W_p + A^{-1}\,C\,Q_p. \qquad (8)
$$

In (8), the matrices A, B, C have the dimension $N \times N$ and A can be written as (9) on the next page where A_1^X with positive integer X is a square $X \times X$ matrix and O is the zero matrix with compatible dimensions. Also in (9)

$$
\begin{aligned}
S &= \frac{1}{\delta_x\,\delta_y^3} + \frac{1}{\delta_y\,\delta_x^3} + \frac{1}{2\,\delta_x^4} + \frac{1}{2\,\delta_y^4} + \frac{\rho}{D\,\delta_t^2}, \\
Q &= \frac{\delta_x\,\delta_y - \delta_y^2 - 2\,\delta_x^2}{4\,\delta_x^5\,\delta_y + 4\,\delta_x^4\,\delta_y^2}, \quad R = \frac{\delta_x\,\delta_y - 2\,\delta_y^2 - \delta_x^2}{4\,\delta_x^2\,\delta_y^4 + 4\,\delta_x\,\delta_y^5}, \\
P &= \frac{1}{2\,\delta_x^2\,\delta_y^2} - \frac{1}{2\,\delta_x\,\delta_y^3} - \frac{1}{2\,\delta_x^3\,\delta_y}
\end{aligned}
$$

Also the matrix B has the same structure as A with

$$
\begin{aligned}
S &= \frac{2}{\delta_x\,\delta_y^3} + \frac{2}{\delta_y\,\delta_x^3} + \frac{1}{\delta_x^4} + \frac{1}{\delta_y^4} - 2\frac{\rho}{D\,\delta_t^2}, \\
Q &= \frac{\delta_x\,\delta_y - \delta_y^2 - 2\,\delta_x^2}{2\,\delta_x^5\,\delta_y + 2\,\delta_x^4\,\delta_y^2}, \quad R = \frac{\delta_x\,\delta_y - 2\,\delta_y^2 - \delta_x^2}{2\,\delta_x^2\,\delta_y^4 + 2\,\delta_x\,\delta_y^5}, \\
P &= \frac{1}{\delta_x^2\,\delta_y^2} - \frac{1}{\delta_x\,\delta_y^3} - \frac{1}{\delta_x^3\,\delta_y}.
\end{aligned}
$$

$$
A=\begin{bmatrix}
A_1^{\frac{n+1}{2}} & A_2 & A_3 & O & \cdots & \cdots & \cdots & \cdots & \cdots\cdots & \cdots & \cdots & O\\
A_2^{\mathrm{T}} & A_1^{\frac{n+3}{2}} & A_2 & A_3 & O & \ddots & \ddots & \ddots & \ddots & \ddots & \ddots & \vdots\\
A_3^{\mathrm{T}} & A_2^{\mathrm{T}} & A_1^{\frac{n+5}{2}} & A_2 & A_3 & O & \ddots & \ddots & \ddots & \ddots & \ddots & \vdots\\
O & \ddots & \ddots & \ddots & \ddots & \ddots & \ddots & \ddots & \ddots & \ddots & \ddots & \vdots\\
\vdots & \ddots & \ddots & \ddots & \ddots & A_3 & \ddots & \ddots & \ddots & \ddots & \ddots & \vdots\\
\vdots & \ddots & \ddots & \ddots & A_1^{n-1} & A_2 & A_4 & \ddots & \ddots & \ddots & \ddots & \vdots\\
\vdots & \ddots & \ddots & A_3^{\mathrm{T}} & A_2^{\mathrm{T}} & A_1^{n} & A_2 & A_3 & \ddots & \ddots & \ddots & \vdots\\
\vdots & \ddots & \ddots & \ddots & A_4^{\mathrm{T}} & A_2^{\mathrm{T}} & A_1^{n-1} & \ddots & \ddots & \ddots & \ddots & \vdots\\
\vdots & \ddots & \ddots & \ddots & \ddots & A_3^{\mathrm{T}} & \ddots & \ddots & \ddots & \ddots & \ddots & \vdots\\
\vdots & \ddots & \ddots & \ddots & \ddots & \ddots & \ddots & \ddots & \ddots & \ddots & \ddots & O\\
\vdots & \ddots & \ddots & \ddots & \ddots & \ddots & O & A_3^{\mathrm{T}} & A_2^{\mathrm{T}} & A_1^{\frac{n+5}{2}} & A_2 & A_3\\
\vdots & \ddots & \ddots & \ddots & \ddots & \ddots & \ddots & O & A_3^{\mathrm{T}} & A_2^{\mathrm{T}} & A_1^{\frac{n+3}{2}} & A_2\\
O & \cdots & \cdots & \cdots\cdots & \cdots & \cdots & \cdots & \cdots & O & A_3^{\mathrm{T}} & A_2^{\mathrm{T}} & A_1^{\frac{n+1}{2}}
\end{bmatrix},\quad
A_1^X=\begin{bmatrix}
S & Q & 0 & \cdots & 0\\
Q & \ddots & \ddots & \ddots & \vdots\\
0 & \ddots & \ddots & \ddots & 0\\
\vdots & \ddots & \ddots & \ddots & Q\\
0 & \cdots & 0 & Q & S
\end{bmatrix},\quad
A_2=\begin{bmatrix}
P & P & 0 & \cdots\cdots & 0\\
0 & \ddots & \ddots & \ddots & \vdots\\
0 & \ddots & \ddots & \ddots & 0\\
\vdots & \ddots & \ddots & \ddots & 0\\
0 & \cdots\cdots & 0 & P & P
\end{bmatrix},\quad
A_3=\begin{bmatrix}
0 & R & 0 & \cdots\cdots & 0\\
0 & \ddots & \ddots & \ddots & \vdots\\
\vdots & \ddots & \ddots & \ddots & 0\\
0 & \cdots\cdots & 0 & R & 0
\end{bmatrix}, \tag{9}
$$

and

$$
A_4=\begin{bmatrix}
R & 0 & \cdots & 0\\
0 & \ddots & \ddots & \vdots\\
\vdots & \ddots & \ddots & 0\\
0 & \cdots & 0 & R
\end{bmatrix},\quad
C=\begin{bmatrix}
1/D & 0 & \cdots & 0\\
0 & \ddots & \ddots & \vdots\\
\vdots & \ddots & \ddots & 0\\
0 & \cdots & 0 & 1/D
\end{bmatrix}. \tag{10}
$$

Note that an alternative way of running simulations is to solve (7) directly by a multigrid algorithm, see (Rabenstein and Steffen, 2012). The node distances in the x and y directions are given by

$$
\delta_x=\frac{a}{n+1},\qquad \delta_y=\frac{\sqrt{3}}{2}\delta_x,
$$

respectively.

4. ILC PROBLEM FORMULATION

Rewrite (8) in the form

$$
W_{p+2}=\hat{A}_1W_{p+1}+\hat{A}_2W_p+\hat{B}Q_p, \tag{11}
$$

where

$$
\hat{A}_1=-A^{-1}B,\qquad \hat{A}_2=-I,\qquad \hat{B}=A^{-1}C. \tag{12}
$$

This is a second-order difference equation and hence to transform it to first-order form introduce

$$
\mathbf{W}_p=\begin{bmatrix}W_{p+1}\\ W_p\end{bmatrix},\ \ \mathbf{Q}_p=Q_p \tag{13}
$$

to obtain the state equation

$$
\mathbf{W}_{p+1}=\mathbf{A}\mathbf{W}_p+\mathbf{B}\mathbf{Q}_p \tag{14}
$$

with $p\geq 0$ and

$$
\mathbf{A}=\begin{bmatrix}\hat{A}_1 & \hat{A}_2\\ I & O\end{bmatrix},\quad \mathbf{B}=\begin{bmatrix}\hat{B}\\ O\end{bmatrix}. \tag{15}
$$

To formulate the ILC design problem, a positive integer variable k denoting the trial-to-trial update in the iteration domain is introduced. Then (14) is written as

$$
\mathbf{W}_{p+1}(k)=\mathbf{A}\mathbf{W}_p(k)+\mathbf{B}\mathbf{Q}_p(k). \tag{16}
$$

Introduce the output equation

$$
\mathbf{Y}_p(k)=\mathbf{C}\mathbf{W}_p(k)=W_{p+1}(k) \tag{17}
$$

with

$$
\mathbf{C}=[I\ \ O]\,. \tag{18}
$$

Also define the tracking error $\mathbf{E}_p(k)$ as

$$
\begin{aligned}
\mathbf{E}_p(k)&=\mathbf{Y}_p^*-\mathbf{Y}_p(k)\\
&=W_{p+1}^*-W_{p+1}(k),
\end{aligned} \tag{19}
$$

where $\mathbf{Y}_p^*$ denotes a spatial/temporal reference signal.

Introduce the state and control increments as

$$
\Theta_{p+1}(k+1)=\mathbf{W}_p(k+1)-\mathbf{W}_p(k) \tag{20}
$$

$$
\Delta\mathbf{Q}_p(k+1)=\mathbf{Q}_p(k+1)-\mathbf{Q}_p(p) \tag{21}
$$

and apply the ILC law

$$
\Delta\mathbf{Q}_p(k+1)=\mathbf{K}_1\,\Theta_{p+1}(k+1)+\mathbf{K}_2\,\mathbf{E}_{p+1}(k) \tag{22}
$$

to obtain the following ILC dynamics written in the form of a discrete linear repetitive process Rogers et al. (2007)

$$
\begin{aligned}
\Theta_{p+1}(k+1)&=\bar{A}\,\Theta_p(k+1)+\bar{B}\,\mathbf{E}_p(k)\\
\mathbf{E}_p(k+1)&=\bar{C}\,\Theta_p(k+1)+\bar{D}\,\mathbf{E}_p(k),
\end{aligned} \tag{23}
$$

where

$$
\begin{aligned}
\bar{A}&=\mathbf{A}+\mathbf{B}\,\mathbf{K}_1, & \bar{B}&=\mathbf{B}\,\mathbf{K}_2,\\
\bar{C}&=-\mathbf{C}\bar{A}, & \bar{D}&=I-\mathbf{C}\bar{B}.
\end{aligned} \tag{24}
$$

Finally, the control signal for (16) can be computed from (22) as

$$
\begin{aligned}
\mathbf{Q}_p(k)=\mathbf{Q}_p(k-1)&+\mathbf{K}_1\left(\mathbf{W}_p(k)-\mathbf{W}_p(k-1)\right)\\
&+\mathbf{K}_2\left(\mathbf{Y}_{p+1}^*-\mathbf{Y}_{p+1}(k-1)\right).
\end{aligned} \tag{25}
$$

5. ILC DESIGN

Introduce the Lyapunov function

$$
\begin{aligned}
V_p(k)=\ &\Theta_p(k+1)^TP_1\,\Theta_p(k+1)\\
&+\mathbf{E}_p(k)^TP_2\,\mathbf{E}_p(k)
\end{aligned} \tag{26}
$$

and the associated increment

$$
\begin{aligned}
\Delta V_p(k)=\ &\Theta_{p+1}(k+1)^TP_1\,\Theta_{p+1}(k+1)\\
&-\Theta_p(k+1)^TP_1\,\Theta_p(k+1)\\
&+\mathbf{E}_p(k+1)^TP_2\,\mathbf{E}_p(k+1)-\mathbf{E}_p(k)^TP_2\,\mathbf{E}_p(k).
\end{aligned} \tag{27}
$$

Using the stability theory for discrete linear repetitive processes (Rogers et al., 2007), ILC trial-to-trial convergence occurs when

$$\Delta V_p(k) \le 0, \quad \forall\, k, p > 0, \tag{28}$$

or

$$\begin{bmatrix} \bar{A}^T P_1 \bar{A} - P_1 + \bar{C}^T P_2 \bar{C} & \bar{A}^T P_1 \bar{B} + \bar{C}^T P_2 \bar{D} \\ \bar{B}^T P_1 \bar{A} + \bar{D}^T P_2 \bar{C} & \bar{B}^T P_1 \bar{B} + \bar{D}^T P_2 \bar{D} - P_2 \end{bmatrix} \prec 0. \tag{29}$$

Introduce

$$\bar{\mathcal{A}} = \begin{bmatrix} \bar{A} & \bar{B} \\ \bar{C} & \bar{D} \end{bmatrix}, \quad \bar{\mathcal{P}} = \mathrm{diag}\,(P_1, P_2) \tag{30}$$

to rewrite (29) in the form

$$\bar{\mathcal{A}}^T \bar{\mathcal{P}} \bar{\mathcal{A}} - \bar{\mathcal{P}} \prec 0, \tag{31}$$

which, however, is not a Linear Matrix Inequality (LMI). Further, rewrite $\bar{\mathcal{A}}$ as

$$\bar{\mathcal{A}} = \begin{bmatrix} \mathbf{A} + \mathbf{B}\mathbf{K}_1 & \mathbf{B}\mathbf{K}_2 \\ -\mathbf{C}\mathbf{A} - \mathbf{C}\mathbf{B}\mathbf{K}_1 & I - \mathbf{C}\mathbf{B}\mathbf{K}_2 \end{bmatrix} \tag{32}$$

and introduce

$$\begin{aligned} \bar{\mathbb{A}} &= \begin{bmatrix} \mathbf{A} & O \\ O & I \end{bmatrix}, \quad \bar{\mathbb{B}} = \begin{bmatrix} \mathbf{B} & \mathbf{B} \\ O & O \end{bmatrix}, \quad \bar{\mathbb{C}} = \begin{bmatrix} I & O \\ -\mathbf{C} & I \end{bmatrix}, \\ \mathbb{K} &= \mathrm{diag}\,(\mathbf{K}_1, \mathbf{K}_2)\,, \quad \mathbb{A} = \bar{\mathbb{C}}\bar{\mathbb{A}}, \quad \mathbb{B} = \bar{\mathbb{C}}\bar{\mathbb{B}} \end{aligned} \tag{33}$$

to obtain (32) in the form

$$\bar{\mathcal{A}} = \mathbb{A} + \mathbb{B}\mathbb{K}. \tag{34}$$

Then, (31) becomes

$$(\mathbb{A} + \mathbb{B}\mathbb{K})^T \bar{\mathcal{P}} (\mathbb{A} + \mathbb{B}\mathbb{K}) - \bar{\mathcal{P}} \prec 0, \tag{35}$$

where $\prec 0$ denotes a symmetric negative definite matrix. Now, the major result of this paper can be established, where $\succ 0$ denotes a symmetric positive definite matrix.

Theorem 1. The discrete linear repetitive process describing the ILC dynamics (23) is stable and ILC trial-to-trial error convergence occurs if there exists $\tilde{\mathcal{P}} \succ 0$, where $\tilde{\mathcal{P}} = \mathrm{diag}\left(\tilde{\mathcal{P}}_1, \tilde{\mathcal{P}}_2\right)$, and $\tilde{\mathcal{N}} = \mathrm{diag}\left(\tilde{\mathcal{N}}_1, \tilde{\mathcal{N}}_2\right)$ such that the LMI

$$\begin{bmatrix} -\tilde{\mathcal{P}} & \tilde{\mathcal{P}}\mathbb{A}^T + \tilde{\mathcal{N}}^T \mathbb{B}^T \\ \mathbb{A}\tilde{\mathcal{P}} + \mathbb{B}\tilde{\mathcal{N}} & -\tilde{\mathcal{P}} \end{bmatrix} \prec 0 \tag{36}$$

is feasible. If this LMI is feasible, the control law matrices $\mathbf{K}_1$ and $\mathbf{K}_2$ in (22) are

$$\begin{aligned} \mathbb{K} &= \tilde{\mathcal{N}}\tilde{\mathcal{P}}^{-1} = \mathrm{diag}\,(\mathbf{K}_1, \mathbf{K}_2) \\ &= \mathrm{diag}\left(\tilde{\mathcal{N}}_1 \tilde{\mathcal{P}}_1^{-1}, \tilde{\mathcal{N}}_2 \tilde{\mathcal{P}}_2^{-1}\right). \end{aligned} \tag{37}$$

Proof 1. An obvious application of the Schur's complement formula to (35) gives

$$\begin{bmatrix} -\bar{\mathcal{P}} & (\mathbb{A} + \mathbb{B}\mathbb{K})^T \\ \mathbb{A} + \mathbb{B}\mathbb{K} & -\bar{\mathcal{P}}^{-1} \end{bmatrix} \prec 0. \tag{38}$$

Next, pre- and post-multiply this last inequality by $\mathrm{diag}\,(\bar{\mathcal{P}}^{-1}, I)$ to obtain

$$\begin{bmatrix} -\bar{\mathcal{P}}^{-1} & \bar{\mathcal{P}}^{-1}\mathbb{A}^T + \bar{\mathcal{P}}^{-1}\mathbb{K}^T\mathbb{B}^T \\ \mathbb{A}\bar{\mathcal{P}}^{-1} + \mathbb{B}\mathbb{K}\bar{\mathcal{P}}^{-1} & -\bar{\mathcal{P}}^{-1} \end{bmatrix} \prec 0. \tag{39}$$

Finally, set $\tilde{\mathcal{P}} = \bar{\mathcal{P}}^{-1}$ and $\tilde{\mathcal{N}} = \mathbb{K}\tilde{\mathcal{P}}$ to obtain (36) and the proof is complete.

6. A NUMERICAL EXAMPLE

The dynamics of the circular deformable mirror is considered with the parameters given in Table 6 and the discretization is undertaken using the regular hexagonal grid detailed in (Augusta et al., 2016).

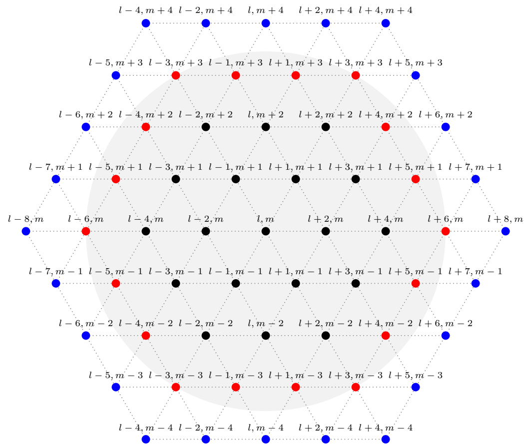

Fig. 2. The circular plate covered by the hexagonal grid with $n = 5$. The deflection at the red points are zero because of the first line of (41). The deflection at the blue points are zero because of (42).

Parameter	Value	Unit
h – thickness	0.01	m
ρ – area density	25	kg m^{-2}
E – Young's modulus	$70 \cdot 10^9$	N m^{-2}
ν – Poisson's ratio	0.22	–

Table 1. Plate Parameters

It is assumed that the edge of the mirror is clamped and hence both the mirror deflection at the edge and its derivative are zero. This leads to the boundary conditions

$$\begin{gathered} w(t, x, y)\Big|_{x,y \in \mathcal{B}} = 0, \\ \frac{\partial w(t, x, y)}{\partial x}\Big|_{x,y \in \mathcal{B}} = 0, \quad \frac{\partial w(t, x, y)}{\partial y}\Big|_{x,y \in \mathcal{B}} = 0, \end{gathered} \tag{40}$$

where $\mathcal{B}$ denotes the boundary of the region where a solution is to be found. Applying the discretization scheme, the conditions of (40) become

$$\begin{gathered} w_{p,l,m} = 0, \\ w_{p,l,m} - w_{p,l-2,m} = 0, \quad w_{p,l,m} - w_{p,l,m-2} = 0 \end{gathered} \tag{41}$$

at boundary nodal points. It follows from (41) that $w_{p,l,m} = 0, w_{p,l-2,m} = 0, w_{p,l,m-2} = 0$ for all p at the boundary nodal points. However, in the simulations, the derivatives (40) are approximated using points on the boundary and outside the region where the solution is sought. Derivatives in the x-direction are approximated by, see Fig. 2, for example,

$$\begin{aligned} w_{p,l-6,m} - w_{p,l-8,m} &= 0 \text{ at } w_{p,l-6,m}, \\ w_{p,l-5,m+1} - w_{p,l-7,m+1} &= 0 \text{ at } w_{p,l-5,m+1}, \\ w_{p,l+4,m+2} - w_{p,l+6,m+2} &= 0 \text{ at } w_{p,l+4,m+2}, \\ w_{p,l-4,m-2} - w_{p,l-6,m-2} &= 0 \text{ at } w_{p,l-4,m-2}, \\ w_{p,l+3,m-3} - w_{p,l+5,m-3} &= 0 \text{ at } w_{p,l+3,m-3}, \end{aligned} \tag{42}$$

etc, with similar approximations for the derivatives in the y-direction. It follows from (42) that the deflection is still zero at all the boundary nodal points and all external nodal points denoted by the red and blue colors, respectively, in Fig. 2. Hence the deflection at these points do not need to be computed.

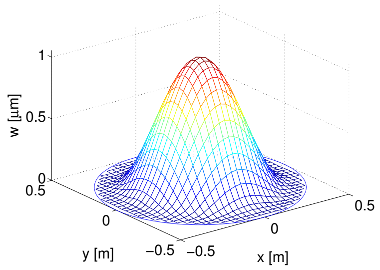

Fig. 3. Reference signal at time instants $t = 4, 5, 6, 7$ s.

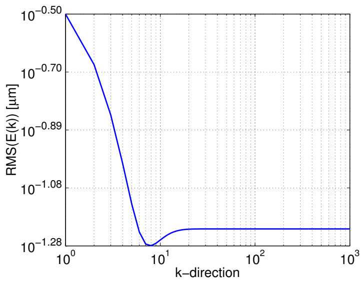

Fig. 4. RMS error for the ILC design.

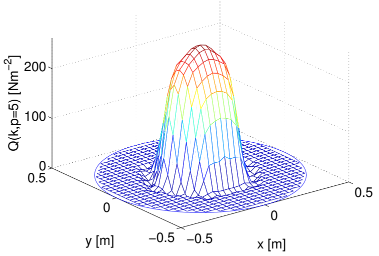

Fig. 5. Control signal at $k = 20$ and $p = 5$.

Consider the diameter of the plate $a = 1$ m and the discretization grid with $n = 11$. These values result in $\delta_x = 0.0833$ m and $\delta_y = 0.0722$ m. Let the sampling period be $\delta_t = 1$ s. The initial conditions are taken as zero values and the duration of the reference signal shown in Fig. 3 is $t_f = 11$ s (discrete time $p = 0, 1, \ldots, 11$). The middle point of the plate corresponds to the maximum value of the reference signal.

Applying Theorem 1 results in the control law matrices $\mathbf{K}_1$ and $\mathbf{K}_2$ of (37) that are not shown here due to their large dimensions ($N \times 2\,N = 91 \times 182$ and $N \times N = 91 \times 91$). Also the Root Mean Square (RMS) error along the trials is defined as

$$\text{RMS}\,(\mathbf{E}(k)) = \sqrt{(\mathbf{E}(k)^T\,\mathbf{E}(k))\,/(\beta\,N)} \qquad (43)$$

and is plotted in Fig. 4, which shows fast trial-to-trial error convergence. In (43), where in this case $\beta = 12$ and hence the control is applied at 19 of the $N = 91$ points: $q_{p,l-2,m+2}, \ldots, q_{p,l,m}, \ldots, q_{p,l+2,m-2}$. The control signal is shown in Fig. 5 on trial $k = 20$ and $p = 5$ where it reaches its maximum value.

7. CONCLUSION

This paper has considered a form of the Crank-Nicolson discretization scheme for a PDE in Lagrange form describing the vibrations of a circular thin plate to construct a discrete model in the form of a singular wave repetitive process as a basis for control design studies. As one possible design, iterative learning control has been considered and illustrated by a numerical example.

REFERENCES

Augusta, P., Cichy, B., Galkowski, K., and Rogers, E. (2015). An unconditionally stable finite difference scheme systems described by second order partial differential equations. In *Proceedings of the 2015 IEEE 9th International Workshop on MultiDimensional (nD) Systems*, 134–139.

Augusta, P., Cichy, B., Galkowski, K., and Rogers, E. (2016). An unconditionally stable approximation of a circular flexible plate described by a fourth order partial differential equation. In *Proceedings of the 21st International Conference on Methods and Models in Automation and Robotics*, 1039–1044.

Cichy, B., Gałkowski, K., and Rogers, E. (2012). Iterative learning control for spatio-temporal dynamics using Crank-Nicholson discretization. *Multidimensional Systems and Signal Processing*, 23, 185–208.

Cichy, B., Gałkowski, K., Rogers, E., and Kummert, A. (2011). An approach to iterative learning control for spatio-temporal dynamics using nD discrete linear systems models. *Multidimensional Systems and Signal Processing*, 22, 83–96.

Crank, J. and Nicolson, P. (1947). A practical method for numerical evaluation of solutions of partial differential equations of the heat-conduction type. *Proceedings of the Cambridge Philosophical Society*, 43, 50–67.

Rabenstein, R. and Steffen, P. (2009). Implicit discretization of linear partial differential equations and repetitive processes. In *Proceedings of the 6th International Workshop on Multidimensional (nD) Systems*, 1–7.

Rabenstein, R. and Steffen, P. (2011). Stability analysis for implicit second order finite difference schemes. In *Proceedings of 7th International Workshop on Multidimensional (nD) Systems (nDs)*, 1–6.

Rabenstein, R. and Steffen, P. (2012). Numerical iterative methods and repetitive processes. *Multidimensional Systems and Signal Processing*, 23(1-2), 163–183.

Rogers, E., Gałkowski, K., and Owens, D.H. (2007). *Control Systems Theory and Applications for Linear Repetitive Processes*, volume 349 of *Lecture Notes in Control and Information Sciences*. Springer.

Strikwerda, J.C. (1989). *Finite difference schemes and partial differential equations*. Belmont: Wadsworth and Brooks.

Timoshenko, S. and Woinowski-Krieger, S. (1959). *Theory of plates and shells*. New York: McGraw-Hill.